IIETA International Information and Engineering Technology Association
Advancing the World of Information and Engineering

Traitement du Signal
Vol. 41, No. 6, December, 2024, pp. 2763-2775
Journal homepage: http://iieta.org/journals/ts

The Blind Equalization Using SOSA-MIMO Algorithm with QOSTBC Coding

Abderrazak Derbale[1,2*], Abdesselam Bassou[1,2]

[1] Department of Electrical Engineering, Tahri Mohamed University of Bechar, Bechar 08000, Algeria
[2] Laboratory of the Information Processing & Telecommunications (LTIT), Tahri Mohamed University of Bechar, Bechar 08000, Algeria

Corresponding Author Email: derbal.abderrazak@univ-bechar.dz

https://doi.org/10.18280/ts.410601

Received: 27 May 2024
Revised: 30 November 2024
Accepted: 13 December 2024
Available online: 31 December 2024

Keywords:
blind equalizer, MIMO-SOSA, QOSTBC, MIMO fading channels, Rayleigh fading channel

ABSTRACT

The adaptive blind equalization with the QOSTBC coding technique over a Multi-input Multi-output (MIMO) transmission channel has become the first choice for increasing spectral efficiency in bandwidth-congested areas nowadays, especially in mobile applications. In this paper, we propose a new adaptive blind equalizer using the second-order statistical algorithm (SOSA) in a MIMO system with QOSTBC coding technique. This association ensures full diversity and maximizes the QOSTBC minimum coding gain distance. The simulation results are presented for MIMO-SOSA under 5G wireless Rayleigh channels so that a fair performance comparison with other reference techniques can be established. The results show that by using MIMO-SOSA along with a coding QOSTBC technique over fading channel a BER at high SNR can be achieved. More importantly, it is also shown that QOSTBC using MIMO-SOSA achieves a better error performance than those using conventional modulation format.

1. INTRODUCTION

In the recent years, many researchers have been conducted on wireless multimedia communication issues, with the growing demand for real-time processing of big data, Internet of Things using artificial intelligence and video streaming; Techniques for increasing throughput in wireless communications coverage at reception are becoming increasingly important [1, 2]. In general, system throughput can be improved by three independent factors: number of transmit antennas and receiver antenna, bandwidth, and spectral efficiency. In particular, the bandwidth limit (capacity) and channel degradation (inter-symbol interference — ISI) are encountered by wireless communication systems. Digital communication over wireless channels can experience severe signal distortion due to the occurrence of multiple paths along the transmission channel. It is not uncommon for nonlinearity at the receiver's analog front-end and the transmitter's high-power amplifier to also impose distortions on the transmitted and received signals. Furthermore, the effects of all these alterations are aggravated by the presence of Additive White Gaussian Noise (AWGN) [3, 4]. Multipath is perhaps the most relevant degradation of digital wireless links [5, 6]. Multipath propagation can cause inter-symbol interference (ISI) [7], compromising the intelligibility of the received signal. Multipath effects are attenuated using channel equalization techniques [8], which essentially implement the

convolution of the channel impulse response [9]. To overcome the problem of ISI caused by multipath propagation in a wireless environment, various coding and channel equalization schemes have been developed. It is recently proposed a new system for equalizing blind channels.

Multi-antenna systems in transmission and reception (Multi-input multi-output MIMO) theoretically allow increasing the capacity of the wireless channel without additional bandwidth, without additional power transmission, or both [10]; compared to systems consisting of a single transmitting and receiving antenna (single input single output SISO). MIMO systems are one of the main axes of development to increase wireless communication speeds although the first works published on this subject, date back only a few years [11-13]. It is witnessing rapid development and this technology has multiple applications in local networks, with or without the Internet, and in communication networks of various generations. MIMO systems have two major advantages over SISO systems. 1- Thanks to the contribution of spatial diversity, they improve the quality of the link by eliminating the discoloration of the channels. 2- They make it possible to increase the flow of information without increasing the bandwidth or the transmitted power. The basic principle of MIMO systems is therefore to judiciously combine the signals on the transmission and on reception to exploit the spatial diversity and reduce the effects of fading, or increase the transmission rate. In this context, when the number of antennas exceeds the number of users, the term massive MIMO (mMIMO) is frequently used. Typically, mMIMO systems operate with 16 or more antennas in base stations (BSs). In addition, the uplink can be composed of one or more UEs, the first characterizing a single-user mMIMO (SU-mMIMO) [14] and the second a multi-user mMIMO (MU-mMIMO) [15]. For new 6G technologies, MIMO schemes have been explored to support terabit data rates [16].

MIMO and mMIMO communications are widely implemented either through bundle formation, space-time block codes (STBC), or both [17, 18]. Because of the diversity gain, they provide to communication systems, space-time orthogonal block codes (STBC) are used to more efficiently exploit the multipath characteristics of the wireless channel [19]. It has been shown, however, that orthogonal codes for complex constellations and more than two transmit antennas cannot achieve a full transmission rate. To solve this problem, Jafarkhani [20] proposed a code structure in which the columns of the transmission matrix are divided into groups. While the columns in a column group are not orthogonal to each other, different column groups are orthogonal to each other. This code structure is known as quasi-orthogonal STBC (QOSTBC) and although such codes guarantee full transmission throughput, they sacrifice full diversity. Su and Xia [21] presented quasi-orthogonal STBCs that achieve full throughput and full diversity.

While beamforming techniques (analog, digital, or hybrid) [22] may be more attractive for BSs, due to the need for many transmit antennas, STBC; on the other hand, can be used in the bath downlink and uplink connections. The combination of modulation system and MIMO is a major trend in mobile communication systems [23, 24], such as 5G and the next generations, which are based on the so-called MIMOOFDM and mMIMO-OFDM [25] approaches. Nevertheless, digital communication systems over wireless channels can experience severe signal degradations due to multipath propagation, additive white Gaussian noise (AWGN) [26, 27], and Doppler effects [28].

The basic principle of MIMO systems is therefore to judiciously combine the signals at transmission and reception to exploit spatial diversity and reduce the effects of fading, or increase the transmission rate. Channel estimation plays an important role in recovering the original signal at the system output. Channel estimation can be done in three ways; they are

1- Estimation of channels based on training;

2- Estimation of blind channels;

3-Semi-blind channel estimation, but blind channel estimation has become popular in digital.

Communication systems due to their ability to improve bandwidth efficiency [29], estimating the channel is problematic. The difficulty of this problem comes from the fact that the input on an unknown channel (the transmitted signal) is not available at the output of the channel (input of the receiver). Solutions to the problem of blind identification can be found in numerous articles [15, 30]. On the other hand, the article [31] presents the results based on second-order statistics. By analyzing the articles [31, 32], we observed that the estimation of the blind channel using second-order statistics can potentially achieve finer performances for an individual than the methods based on second-order statistics of second-order. This type of approach is called blind equalization.

Conventional carrier equalization and recovery algorithms to minimize the mean square error (MSE) in digital communication systems generally require an initial learning period during which a known data sequence is transmitted and correctly synchronized at the level of the receiver [21, 22, 10, 33]. On the other hand, blind channel equalization allows recovering the symbol of an unknown input sequence on the remote channel without using training bits. Also, the equalization of blind channels has become an important topic in digital communications [22]. Blind methods use the sequence of the received signal and some prior knowledge of the input sequence statistics [34]. Non-minimal phase channel equalization has been achieved using high-order statistical methods [35] or other non-linearity which are only effective with non-Gaussian distribution input sequences [36]. According to the study, there are well-known algorithms for the equalization of blind channels, these algorithms, like CMA, FSCMA, and SKMAA [37], are based on adaptive filtering techniques. One new the algorithms, which are based on an MMSE method. The result of this algorithm is better compared to CMA, FS-CMA, and SKM [38, 39]. In this work, we use artificial intelligence to compensate for the lack of information at the reception concerning unknown channel coefficients, as well as the lack of training sequence. And, we propose a new algorithm; this algorithm is MIMO-SOSA (MIMO Second Order Statistic Algorithm). MIMO-SOSA is one of the promising schemes for this. MIMO-SOSA enables an impressive increase in data throughput and capacity in a wireless link without consuming additional energy or bandwidth. This also allows a significant reduction in the complexity of the system. The rest of this work is organized as follows.

The remainder of this work is organized as follows. In Section 2, a brief review of multi-antenna systems is presented. The proposed STBC coding scheme and the QOSTBC coding are presented in Section 3. In Section 4, will be analyzed the MIMO-SOSA blind equalization algorithms with STBC coding for channel estimation and signal detection in MIMO systems. In the next section, the equalizer MIMO-SOSA with and without QOSTBC is simulated and compared with those obtained using OSTBC maximum likelihood decryption. The results are presented in Section 6 and discussed. Finally, the effectiveness of the MIMO-SOSA equalizer evaluation is concluded.

2. MIMO WIRELESS TRANSMISSION

For a MIMO system with t transmit and r Receive antennas, as shown in Figure 1, the received signal $x_{k,m}$ at time instant k and antenna m is given by:

$$x_j = \sum_{i=1}^{N} h_{i,j} c_i + n_j \tag{1}$$

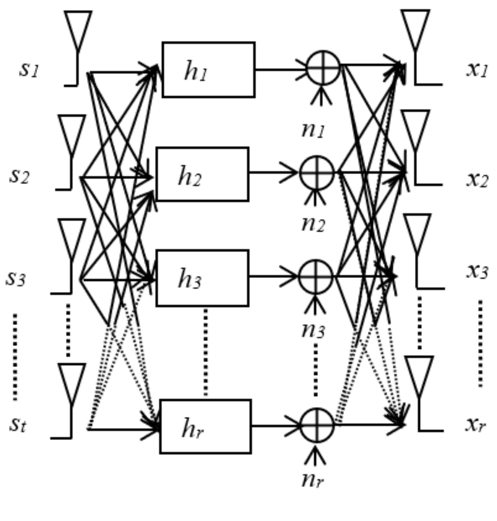

Figure 1. MIMO wireless transmission system

The coefficients $h_{i,j}$ is the gain of the channel between the transmitting antenna i and the receiving antenna j, and n_j is the additive noise, which is modeled on the independent samples and according to a centered Gaussian law of variance $N_0/2$.

Consider the matrix of the MIMO channel H of dimension rxt as follows:

$$H = \begin{bmatrix} h_{11} & \dots & h_{1r} \\ \vdots & \ddots & \vdots \\ h_{t1} & \dots & h_{tr} \end{bmatrix}$$

$$x = Hc + n$$

where, x and n are respectively the receiver and noise vectors of dimension r×1.

2.1 Deterministic MIMO channel capacity

In the MIMO system which employs multiple antennas in the transmitter and/or receiver, the correlation between transmit and receive antenna is an important aspect of the MIMO channel. It depends on the angle of arrival (AoA) of each multi-path component. The study [40] gives a good explanation of how to calculate the capacity of a mono channel. We can determine the capacity of a MIMO channel by the following relation:

$$C = log_2\left(det\left(I_r + \frac{E_s}{tN_0}HH^H\right)\right) \tag{2}$$

where, E_s is the energy of the transmitted signals, and N_0 is the power spectral density of the additive noise, I_r is the unity matrix for rxr, and (^{H}) denotes conjugal.

2.2 Rayleigh fading channel

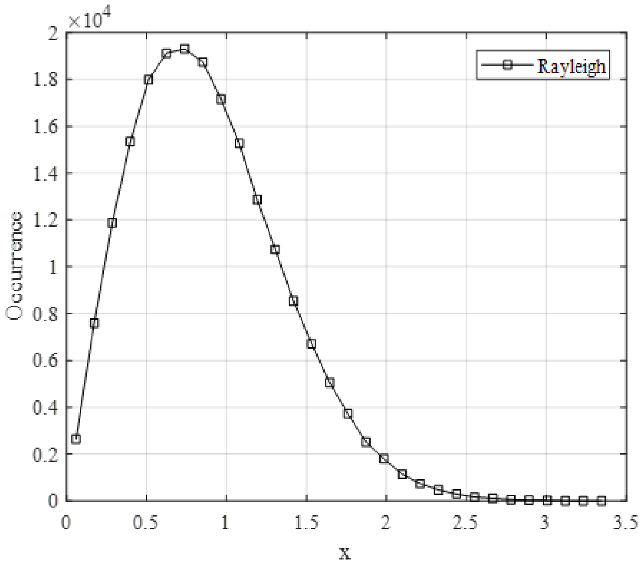

Figure 2. Distributions for Rayleigh fading channels

Rayleigh fading is caused by multipath reception. The mobile antenna receives a large number, say N, of reflected and scattered waves. Because of wave cancellation effects, the instantaneous received power seen by a moving antenna becomes a random variable, dependent on the location of the antenna. Rayleigh fading is a reasonable model when many objects in the environment scatter the radio signal before it arrives at the receiver. The central limit theorem holds that, if there is sufficiently much scatter, the channel impulse response will be well-modeled as a Gaussian process irrespective of the distribution of the individual components. If there is no dominant component to the scatter, then such a process will have zero mean and phase evenly distributed between 0 and 2π radians. The envelope of the channel response will therefore be Rayleigh distributed is shown in Figure 2. Then, note that X is a Rayleigh random variable with the following probability density function (PDF):

$$f_X(x) = \frac{x}{\sigma^2}e^{\frac{-x^2}{2\sigma^2}} \tag{3}$$

3. CRITERIA FOR CONSTRUCTING SPACE-TIME BLOCK CODES

3.1 STBC code

In this paragraph, we will introduce the criteria used for good Space-Time Block codes. Its MIMO system is composed of t transmit antennas and r receive antennas. On transmission, the information symbols s_i that belong to the alphabet Λ_s are grouped in the block and are encoded by the encoder which associates $s = [s_1, s_2, \dots, s_Q]^T$ with the following code matrix of dimension t×T.

$$C = \begin{bmatrix} c_{11} & \cdots & c_{1T} \\ \vdots & \ddots & \vdots \\ c_{N_t1} & \cdots & c_{N_tT} \end{bmatrix}$$

where, the symbol code c_{ij} belongs to the alphabetΛ_s. The yield of the MIMO code is equal to $R_{MIMO} = Q/t$. We can write the following matrix relation:

$$X = HC + N \tag{4}$$

where, X and N are the reception and noise matrices of dimension r×T respectively.

Space-Time codes are divided into two families: Space-Time Trellis (STT) and Space-Time Block (STB) codes. STT codes are a generalization of trellis code modulations to MIMO channels. Although the performance obtained by these codes is excellent, the complexity of the decoding is exponential with the yield. Indeed, in this work, we will present only the block space-temporal codes, which are more interesting at the practical level of performance.

3.2 STBC from Quasi-Orthogonal design (QOSTBC)

For the case t=2 and r=2, Alamouti [19] proposed a Spatiotemporal code with Q=T=2 and therefore RMIMO=1. At time 1, the symbols s1 and s2 are transmitted respectively on antennas 1 and 2, and then at time 2, the symbols -s*2 and s*1 are transmitted on antennas 1 and 2. Thus, in matrix form, we have

$$G_{s_1s_2} = \begin{pmatrix} s_1 & s_2 \\ -s_2^* & s_1^* \end{pmatrix} \tag{5}$$

Then, for four transmit antennas Jafarkhani expanded the Alamouti scheme to:

$$C = \begin{pmatrix} G_{s_1 s_2} & G_{s_3 s_4} \\ -G^*_{s_3 s_4} & G^*_{s_1 s_2} \end{pmatrix} \tag{6}$$

Jafarkhani [20] proposed a quasi-Orthogonal coding scheme using four antennas and consequently four encoded symbols; it is shown in Figure 3. From 4 and 5, it follows that:

$$C_{QOSTBC4} = \begin{pmatrix} s_1 & s_2 & s_3 & s_4 \\ -s_2^* & s_1^* & -s_4^* & s_3^* \\ -s_3^* & -s_4^* & s_1^* & s_2^* \\ s_4 & -s_3 & -s_2 & s_1 \end{pmatrix} \tag{7}$$

where, C is the Quasi-Orthogonal coding matrix. Nevertheless, due to the relaxation of the code orthogonality requirement, decoding complexity increases concerning that of orthogonal codes because only pair-wise decoding is possible. Specifically, decoding by QOSTBC encoded signals is reduced and, to minimize the cost function over [41-43], the information is recovered by the QOSTBC system, the binary, using a MIMO-SOSA-N algorithm that is proposed in this work.

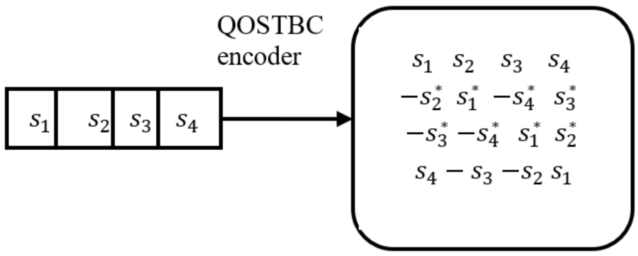

Figure 3. Coding scheme for QOSTBC code

4. BLIND EQUALIZATION ALGORITHM

4.1 Blind equalization algorithm descriptions

The blind equalizer MIMO-SOSA discussed in this section is illustrated in Figure 4. After each channel output, a MIMO filter was used. The filter coefficients are adjusted to minimize the Godard cost function considering the blind equalizer as shown in Figure 4. If we adjust the equalizer parameters for each channel to minimize the Godard cost function in 16, then according to the analysis of this section; the equalizer output x_1 and x_2 ... x_r will be one of the input signals but we do not know which of the input signals. Hence, to develop an algorithm that can simultaneously recover all input signals, we may have to modify the Godard cost function.

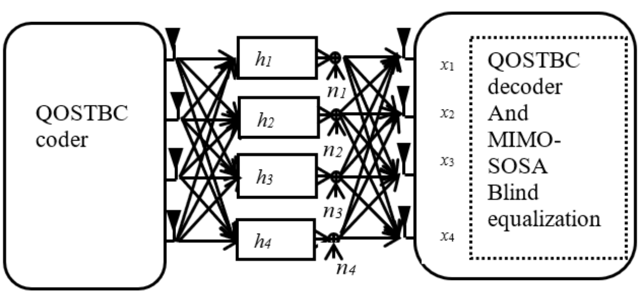

Figure 4. MIMO model system with channel estimation

Blind equalization needs to recover $s(n)$ from $x(n)$ without any explicit knowledge of H and $s(n)$. Only the structure of the statistics is known. In this paper, we focus on the development of blind equalizers because of their simplicity.

For blind equalization, denote G as the matrix operating as an equalizer. The equalizer output is generated from:

$$\hat{S} \equiv GHS$$
$$G = \begin{bmatrix} g_{11} & \cdots & g_{1t} \\ \vdots & \ddots & \vdots \\ g_{r1} & \cdots & g_{rt} \end{bmatrix} \tag{8}$$

where, g_{ij} is the equalizer coefficient.

Consider the blind equalizer shown in Figure 4. If we modify the equalizer parameters for each channel by minimizing the Godard cost function in (10), then at the inputs of the equalizer we find x_1 to x_i but we do not know which of these signals will enter in number one input or in other input. Note that x_1 and x_i are either the same or different from each other depending on the initial setup of the equalizer. Hence, to develop an algorithm that can simultaneously recover all input signals, we may have to modify the Godard cost function.

$$C_{\hat{s},s} = \int_{-\infty}^{+\infty} (p_{\hat{s}}(z) - p_s(z))^2 dz \tag{9}$$

The cost function C is determined by the following formula:

$$C = \frac{1}{pq} E\left[\left||\hat{S}(n)|^p - Q\right|^q\right] \tag{10}$$

where, $Q = \frac{E[S(n)^{2p}]}{E[S(n)^p]}$, and p, q are positive integer parameters.

In this section, we will investigate the performance of the SOSA blind equalizer used in MIMO channels. The idea of this approach is to measure the difference between two the probability density function $p_{\hat{s}}(z)$ and $p_s(z)$ [15, 29].

$$\hat{g}^{k+1} = g^k - \mu R_X^H \varphi(n) \tag{11}$$

where,

$$\varphi(n) = \tfrac{1}{4} \nabla_g C \tag{12}$$

It updates equalizer coefficients by minimizing the cost function. The steepest gradient algorithm is obtained by taking the instantaneous gradient of C which results in an equation that updates the system [30].

$$\varphi(n) = \nabla_g \frac{1}{pq} E\left(\left[\left||\hat{S}(n)|^p - Q\right|^q\right]\right) \tag{13}$$

$$\varphi_i(n) = \partial_{g_i} \frac{1}{pq} E\left(\left[\left||\hat{S}(n)|^p - Q\right|^q\right]\right) \tag{14}$$

$$\varphi_i(n) = \frac{1}{pq} \partial_{g_i} \sum_{i=0}^{r} \left(\left[\left||\hat{S}(n)|^p - Q\right|^q\right]\right) \tag{15}$$

$$\varphi_i(n) = \frac{1}{pq} \partial_{g_i} \sum_{i=0}^{r} ([||\hat{s}_i(n)|^p - Q_i|^q]) \tag{16}$$

with,

$$\hat{S}(n) = GHS(n) \quad (17)$$

$$\hat{s}_i(n) = g_i H s_i \text{ and } Q_i = \frac{E[s_i(n)^{2p}]}{E[s_i(n)^p]}$$

$$\varphi_i(n) = \sum_{i=0}^{p} ([||\hat{s}_i(n)|^p - Q_i|^{q-1}]|\hat{s}_i(n)|^{p-1}(s_i H)^H) \quad (18)$$

For $p = 2$ and $q = 2$, the filter coefficient is adjusted to minimize the Godard cost function [25] for

$$C = \frac{1}{4} E\left[\left|\left|\hat{S}(n)\right|^2 - Q\right|^2\right] \quad (19)$$

$$C_0 = E\left[\left|\left|\hat{S}(n)\right|^2 - Q\right|^2\right] \quad (20)$$

where, the dispersion Q is constantly defined as $Q = \frac{E[S(n)^4]}{E[S(n)^2]}$. Q is a fixed constant, chosen for each form of modulation scheme, represents the statistics of the transmitted signal.

It blindly equalizes the coefficients by the cost function. The steepest gradient descent algorithm is obtained by instantaneous $C_{SOSA\text{-}N}$ which results in the equation updating the system.

$$\varphi_i(n) = \sum_{i=0}^{r} ([||\hat{s}_i(n)|^2 - Q_i|]|\hat{s}_i(n)|(s_i H)^H) \quad (21)$$

$$\hat{g}_i^{k+1} = g_i^k - \mu R_X^H \varphi_i(n) \quad (22)$$

The MIMO-SOSA Algorithm

Previous studies on the blind equalizer used in MIMO can recover one of the input signals and suppress the interference and the rest of the input signal. In this proposal, a new blind equalizer algorithm MIMO-SOSA can recover all input signals simultaneously Without loss of generalization, suppression, and elimination of all kinds of ISI interference and suppression of CCI (co-channel interference) and ACI (adjacent-channel interference). We will assume in this work that the number of transmitter antennas is 3 and 2 respectively, and the transmitter and receiver antennas are 3 and 2 respectively. The number of antennas in the transmitter and receiver can also be increased because the proposed algorithm does its work easily. It results in the equalizers $\hat{s}_1$; $\hat{s}_2$ and $\hat{s}_3$ will be one of the input signals but we do not know which of the input signals. Note that $\hat{s}_1$; $\hat{s}_2$ and $\hat{s}_3$ are either the same or different from each other depending on the equalizer's initial setup. And then, to develop an algorithm that can retrieve all the input signals at one time, where the algorithm separates the signals from each other in a quick way, depending on the recursive system and the comparison between the signals, which is illustrated in this algorithm Figure 5 and Figure 6. The new algorithm MIMO-SOSA for the adaptive blind equalizer of channels is given.

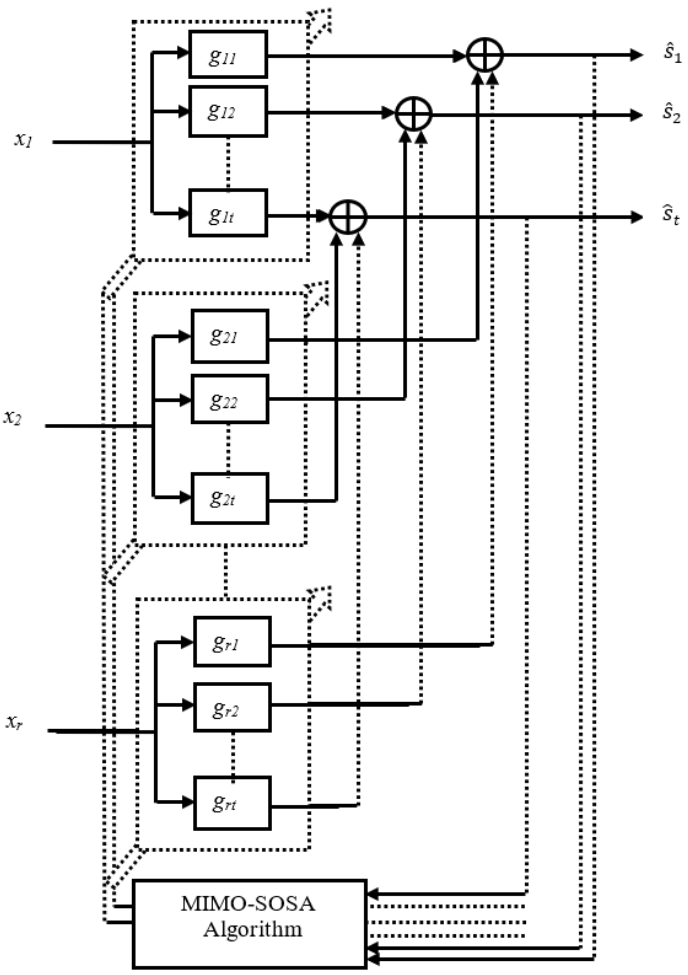

Figure 5. Signal flow graphical representation of the SOSA algorithm for MIMO system

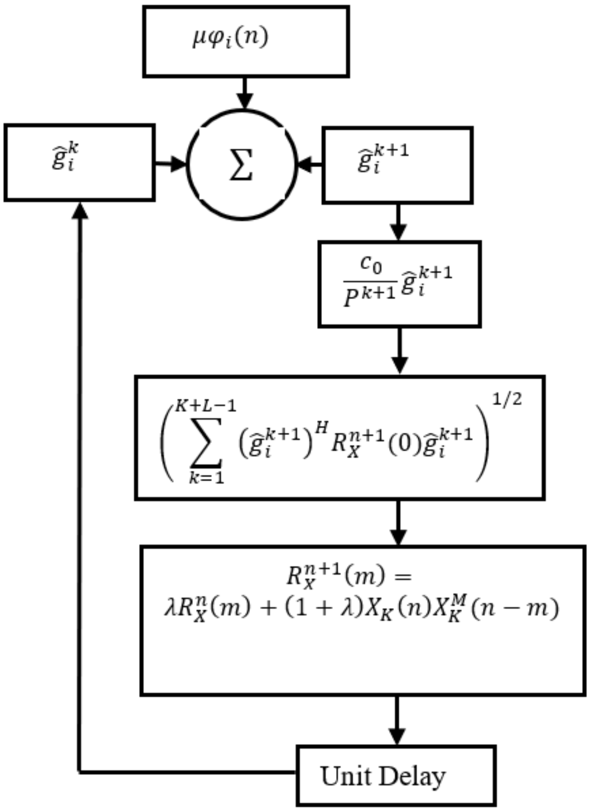

Figure 6. MIMO-SAOA algorithm

Finally, the MIMO-SOSA algorithm for MIMO systems can be determined as follows:

1- Initialize the algorithm by setting $\hat{g}_1^1 = 0$
2- For *i*=1,2…*r*
3- For k=1,2…*t*
4- Where μ is a small step-size λ is a forgetting factor close to 1 [44]
5- $\hat{g}_1^{k+1} = g_i^k - \mu\varphi_i(n)$
6- $g_i^{k+1} = \frac{c_0}{P^{k+1}}\hat{g}_i^{k+1}$
7- $P^{n+1} = \left(\sum_{k=1}^{K+L-1}\left(\hat{g}_i^{k+1}\right)^H R_X^{n+1}(0)\hat{g}_i^{k+1}\right)^{1/2}$
8- $R_X^{n+1}(m) = \lambda R_X^n(m) + (1+\lambda)X_K(n)X_K^H(n-m)$
9- Continue the computation until steady-state conditions are reached
10- Computed

5. SIMULATION

In this simulation, to confirm the analysis results and illustrate the effectiveness of the proposed algorithm, will be present computer simulations with Matlab simulations were performed to compare the performance of BER using a MIMO system for several channels we compare and evaluate this algorithm model according to the evolution of the coefficients of the communication channels, and the number of channels that the signals cross, knowing that at the reception level we do not know the coefficients of these channels and we do not know the learning sequence. Finally, this simulation will use the convergence of this blind equalizer.

In this paper, by adjusting the transmission power for each antenna, the received signals are normalized by the transmission antenna t and by the reception antenna r. For the sake of comparison, the BER as a function of SNR (dB) is used in the simulation. MIMO-SOSA's BER performance in this simulation with one, two, three, and four antennas to the transmitter and receiver has been studied with respect (SISO and MIMO). These channels used in this research are –MIMO fading channels (H(0) and H(1) [32] and MIMO channels used in books (it is well detailed [45]) and Rayleigh fading channels. It will also be assumed that the channel coefficients are constant during code and, will be unknown at the receiver.

In the first part of the simulation (Figure 7), the binary input data is created by a pseudo-random generator with uniform distribution. The bit-stream is then modulated according to the M-PSK modulation scheme used in the simulation. They are transmitted with the help of *t* antenna. On the receiver side, after the transmitted signals pass through the MIMO channels. In the detection, the proposed MIMO-SOSA algorithm blind equalizer technique presented in section 4 is employed to assess the system performance. In the sequel, the detection output symbols are demodulated, BER is computed.

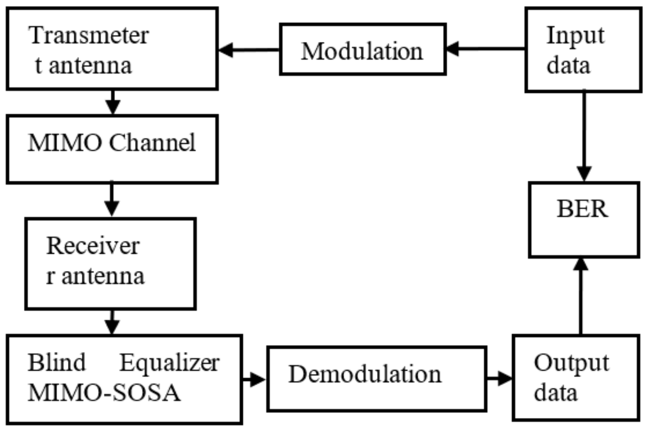

Figure 7. Blok model of simulated system

In the second part of the simulation (Figure 8), the bit-stream in input data is modulated to the M-PSK modulation scheme used in the simulation, then, the modulated symbols are encoded in the QOSTBC block. The transmitted signal passes through the channels and will add centered Gaussian white noise. At the receiver detecting and decoding the signal transmitted with the MIMO-SOSA algorithm presented in this article are employed to assess the system performance. Finally, the detector and decoder output are demodulated, and BER is calculated.

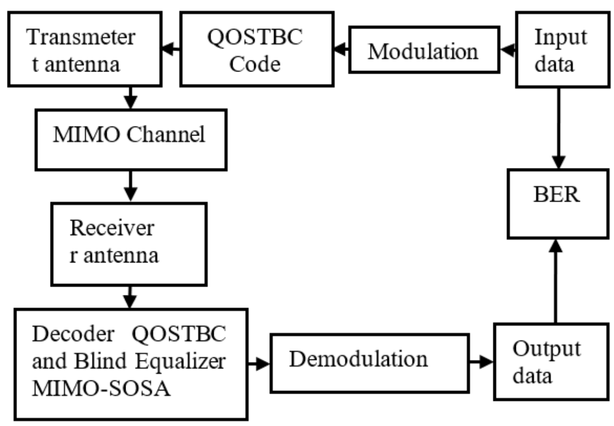

Figure 8. Block model of the simulated system with QOSTBC code

6. RESULTS AND DISCUSSION

The results of simulation are observed and discussed in this section. The system is in a state of interruption if it is not possible to make the decoding error probability arbitrarily small at a transmission rate of Rbps/Hz. Thus, the outage channel capacity is defined as the largest possible data rate such that the outage probability [41] is less than ε = 0.01. In this simulation, we can produce the cumulative distribution function (CDF) of the capacity for the random MIMO channel when CSI is not available at the transmitter side. The Figure 9a shows the CDFs of the random 2×2 and 4×4 MIMO and Figure 9b shows the CDFs of the random 4×4 and 8×8 channel capacities when SNR is 10dB, in which ε =0.01-outage capacity is indicated. It is clear from Figure 9a and Figure 9b that the MIMO channel capacity improves with increasing the number of transmit and receive antennas. Figure 10a and Figure 10b shows the ergodic channel capacity as varying the number of antennas, under the same conditions as for Figure 9a and 9b.

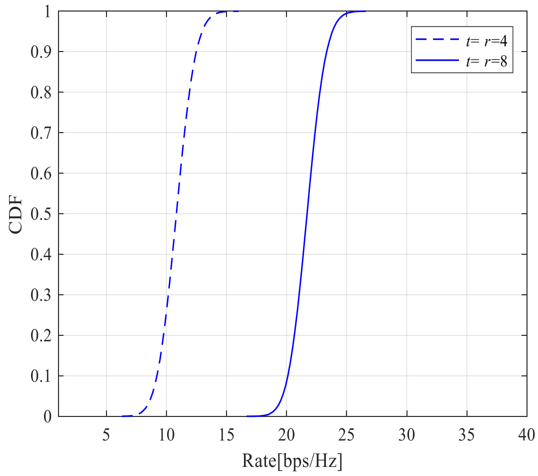

(a)

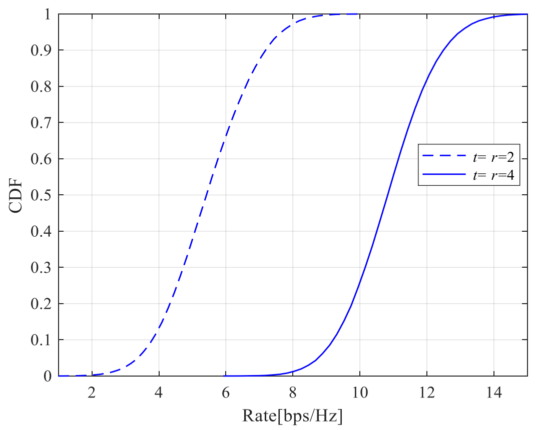

(b)

Figure 9. Distribution of MIMO channel capacity (SNR = 10dB)

Figures 11-13 show the performance of bit error rate (BER) in the SNR function, for Rayleigh channels, with different numbers of antennas using the blind equalization with algorithm MIMO-SOSA. We see that with the increase of the factor SNR, the error coefficient becomes smaller than 10^{-3}, and this contributes to improving communications, and this is even though when receiving, the receiver is completely unaware of his knowledge of each of the coefficient of channel and learning sequence; will be engaging in simulation, At this experience, we applied the principle of blind equalization in the true sense. When using a different number of transmitting and receiving antennas and using Rayleigh channels as shown in the Figure 13, the quality of the communication improves with an increase in the number of antennas, whether for reception or transmission.

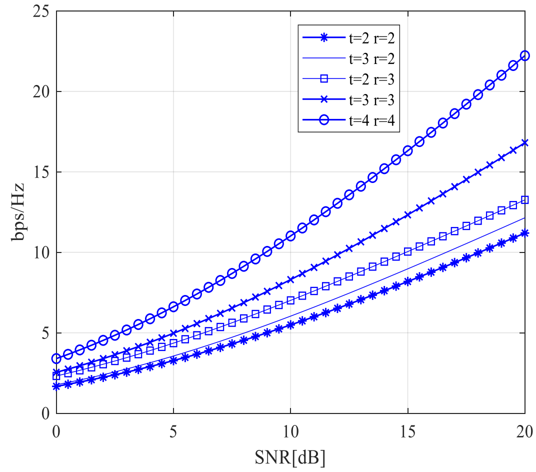

(a)

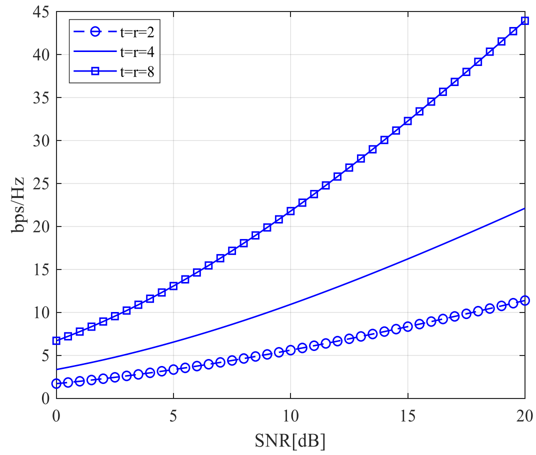

(b)

Figure 10. Ergodic MIMO channel capacity

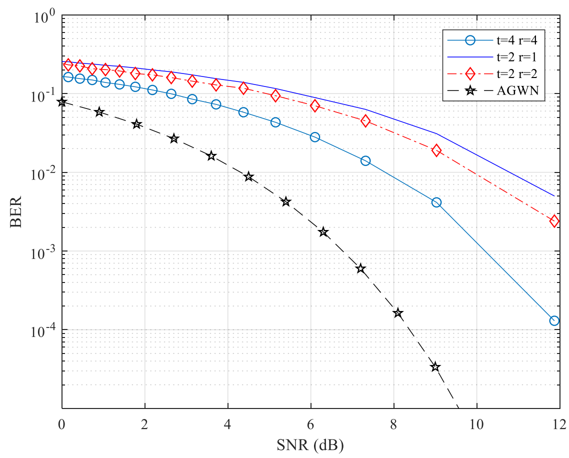

Figure 11. Comparison of the MIMO-SOSA algorithm for Rayleigh fading channels of t = 2 r = 2 and t = 4 r = 4

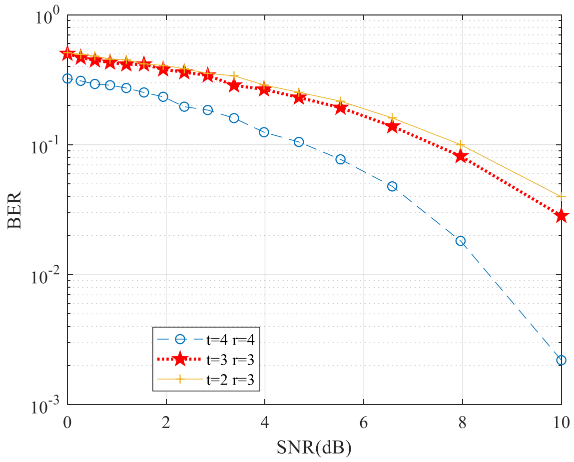

Figure 12. Comparison of the MIMO-SOSA algorithm for Rayleigh fading channels of t = 4 r = 4, t = 3 r = 3, and t = 2 r = 3

For example, when using 8 transmitting antennas and 8 receiving antennas, the superior performance is 2 dB over Using 4 transmitting antennas and 4 receiving antennas, and when using 4 transmitting antennas and 4 receiving antennas, the superior performance is 4 dB over Using 2 transmitting antennas and 2 receiving antennas, this is for BER = 10^{-3}, and this is done using blind equalization. Here we conclude that increasing the number of antennas helps improve the quality of communications, and this is always the case with the use of the MIMO-SOSA Algorithm. We can verify that the blind equalization that used the MIMO-SOSA algorithm for Rayleigh channels provides high-quality performance.

This equalizer improves the quality of communications in all cases studied and is evidence of its effectiveness in communications. In Figure 14 showing a comparison of the performance of $BER = f(SNR)$ for different channel structures, we can verify that the blind equation that used the MIMO-SOSA algorithm for Rayleigh, MIMO fading channel and channel MIMO model [41] (H(0) H(1) [31]), channels gives our convergence between them and high-quality performance. Using blind equalization in all cases studied, this result shows their effectiveness in communications systems.

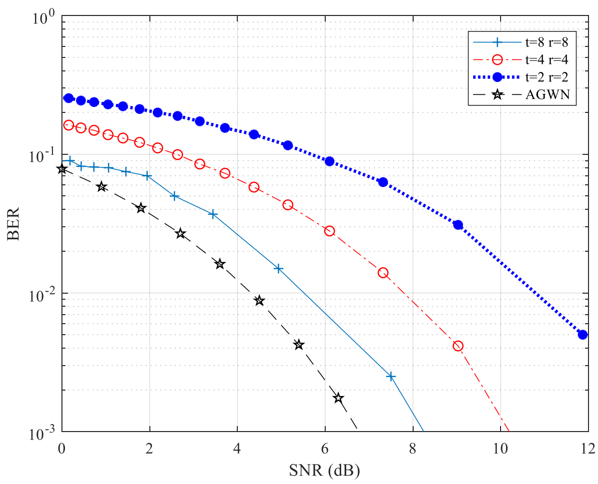

Figure 13. Comparison of the MIMO-SOSA algorithm for Rayleigh fading channels of t = 8 r = 8, t = 4 r = 4; and t = 2 r = 2

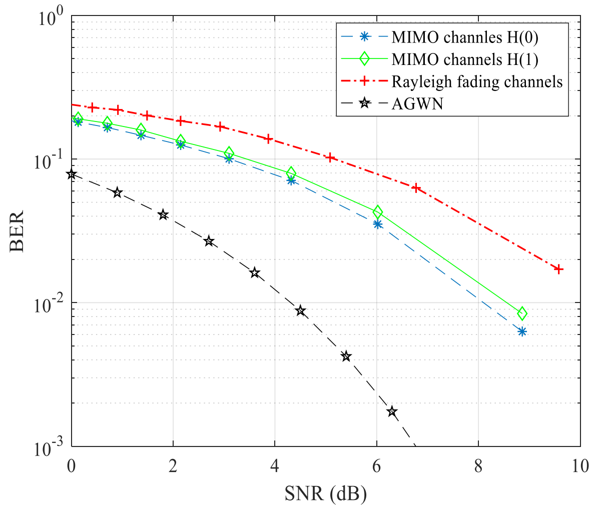

Figure 14. Comparison of the MIMO-SOSA algorithm for MIMO fading channel (H(0); H(1)) and Rayleigh channels of t = 3 r = 2

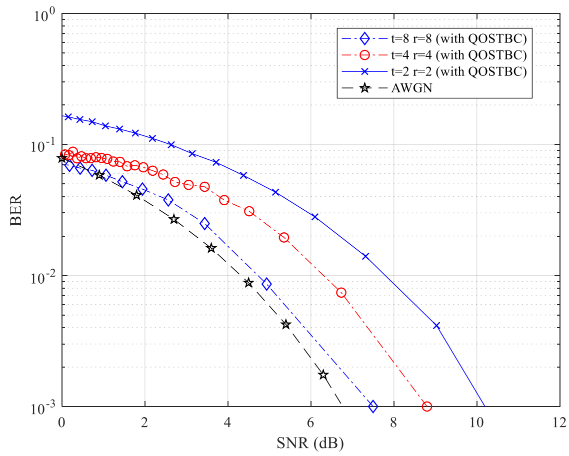

Figure 15. The comparison of the MIMO-SOSA algorithm with QOSTBC code for Rayleigh fading channels with (t = 8 r = 8 t = 4, r =4 and t = 2 r = 2)

In Figure 15, the bit error rate (BER) as a function of SNR for the MIMO-SOSA algorithm using different channels with QOSTBC coding is shown. It can be observed that the MIMO-SOSA algorithm with a Gaussian channel exhibits a higher diversity order compared to any other channel. Additionally, it can be seen that the performance of Rayleigh fading channels provides better results. It can be observed that this algorithm also does a good job on the parameters to compensate for the effect of the channels. There, it can be seen that the system with t = 8 and r = 8 displays a higher diversity order for any other number of antennas, and the communication quality is better than using a smaller number Specifically, we can notice that the system using the number of antenna important constellation has the low BER for high values of signal-to-noise ratio (SNR), for the number of antennas equal to (t = 8 r = 8) we notice that there is a difference in SNR equal to 1.2 dB for BER equal 10^{-2}. The latter (t = 4 and r = 4) gives us more quality for the number of antennas equal to (t = 2 and r = 2). The increase in the number of antennas has given an improvement in the quality of wireless communication.

In Figure 16, the effect of the number of reception and transmission antennas on the quality of wireless communications is studied and compared using the MIMO-SOSA algorithm with OSTBC, as discussed in study [45]. We compared this work to the results in that study to clarify its value and effectiveness. We notice through the comparison that using this algorithm (SOSA-MIMO) is better than the results in that study, and this is from two aspects. First, the equalizers used in study [45] depend on knowing the training sequence or the channel coefficients, unlike the SOSA-MIMO algorithm, which does not depend on knowing the training sequence, and coefficients or the channel coefficients. On the other hand, the SOSA-MIMO algorithm allows for the use of less energy and memory because it does not depend on prior knowledge of the training sequence and channel coefficients.

In Figure 17, the curves comparing the changes in BER as a function of SNR are presented for the MIMO-SOSA algorithm with QOSTBC coding and the MIMO-SOSA algorithm with simple coding. It is observed that as the SNR increases, the BER decreases. Furthermore, the use of the MIMO-SOSA algorithm with QOSTBC coding provides better results and a lower BER compared to the MIMO-SOSA algorithm with simple coding. Will be concluded that the use of the algorithm with the QOSTBC code gives better results than the method which depends on the algorithm using the simple code. In the case of use of the algorithm with QOSTBC for two antennas in transmission and two antennas in reception, it matches the case of use of the algorithm with simple coding for t = 4 and r = 4 antennas. These results show the effectiveness of this blind equalization with QOSTBC coding which proves the advantage of use in wireless communications.

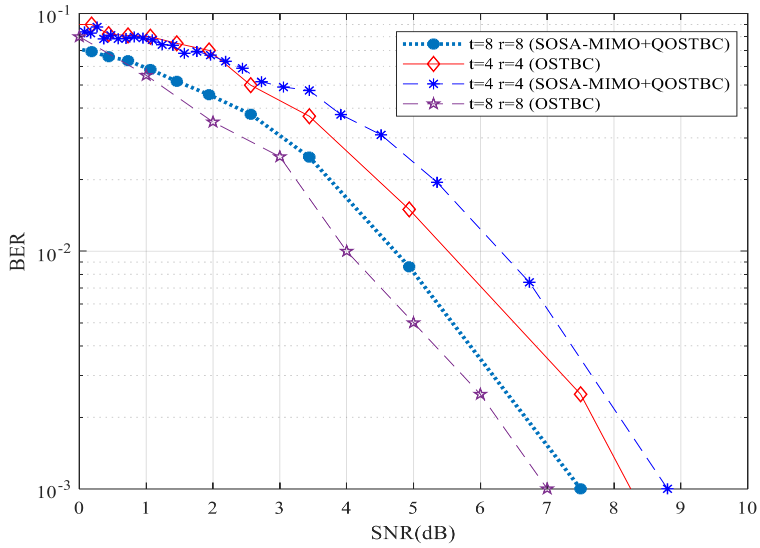

Figure 16. The comparison of the MIMO-SOSA algorithm with OSTBC code for (t = 4, r = 4), and (t = 8, r = 8) for Rayleigh fading channels

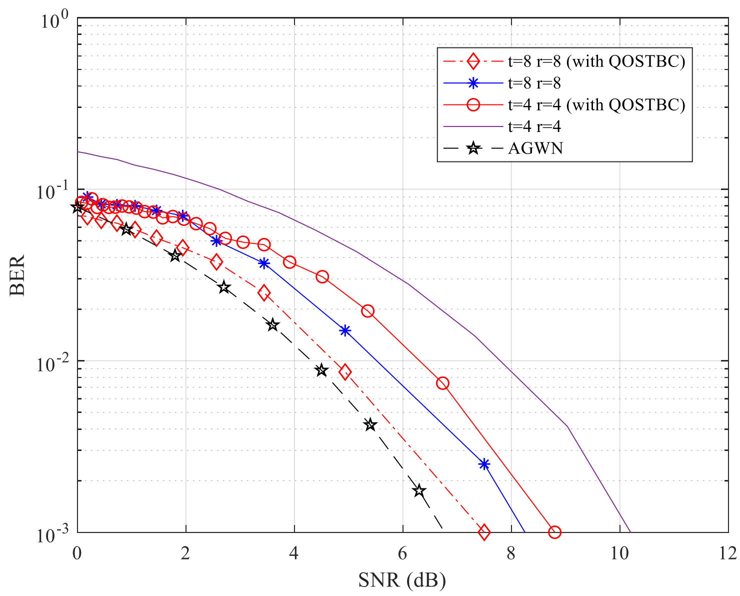

Figure 17. The comparisons of the curves which represent the changes in BER as a function of the SNR with the use of the MIMO-SOSA algorithm with QOSTBC coding and use of the MIMO-SOSA algorithm with simple coding for Rayleigh fading channels

The convergence of SOSA-MIMO Algorithm

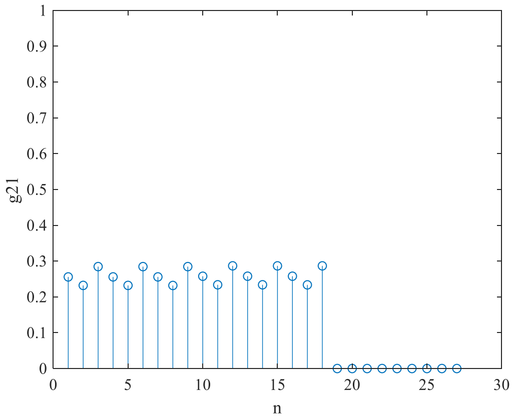

.

(a)

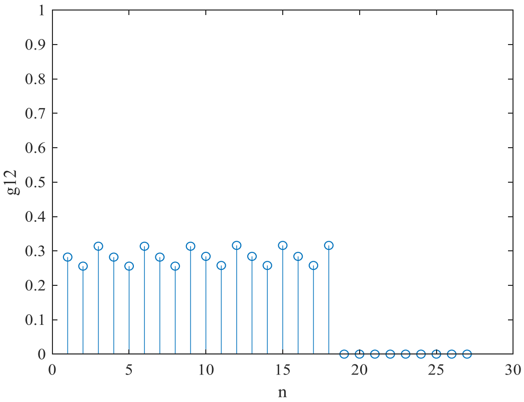

(b)

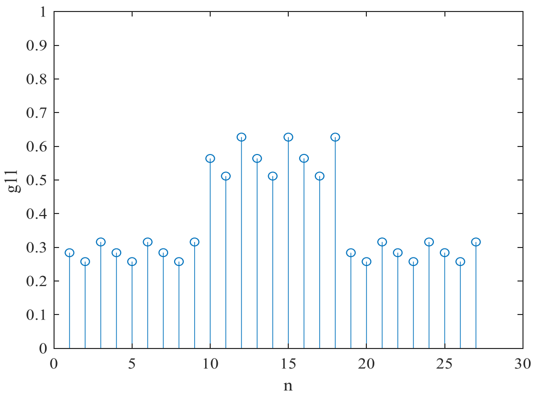

(c)

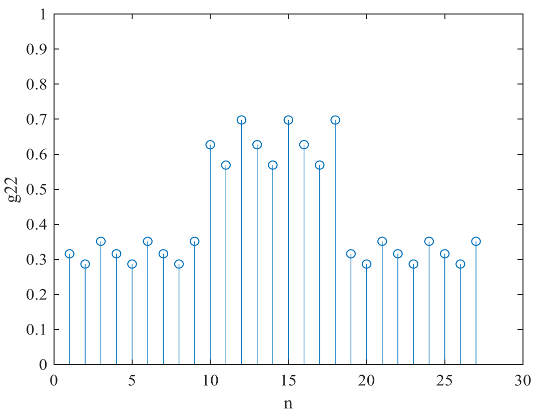

(d)

Figure 18. The impulse response of the equalizer system after 10000 iterations

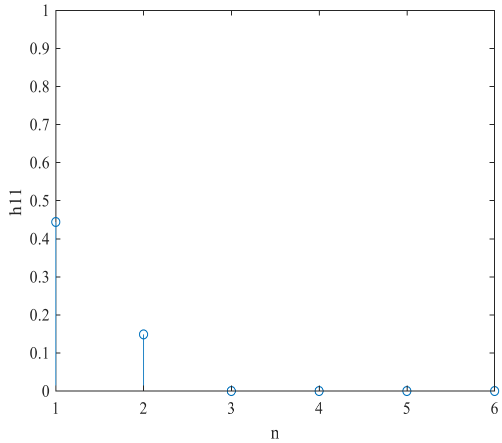

(a)

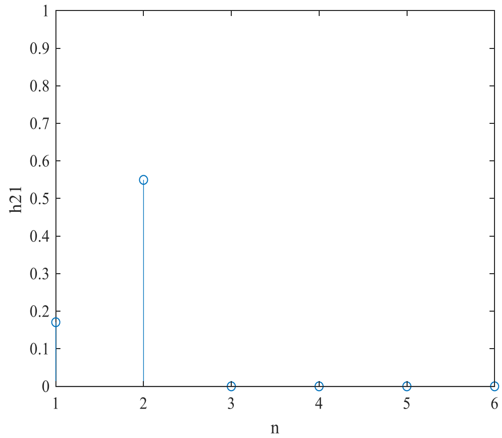

(b)

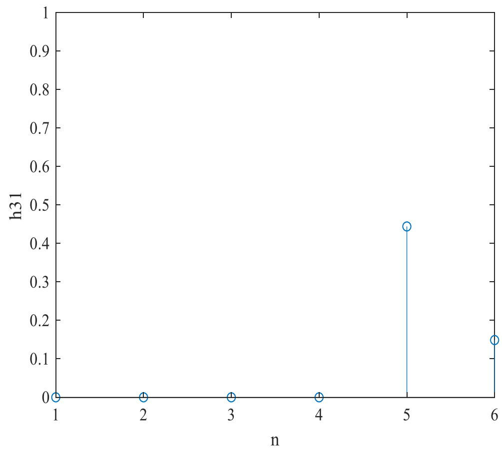

(c)

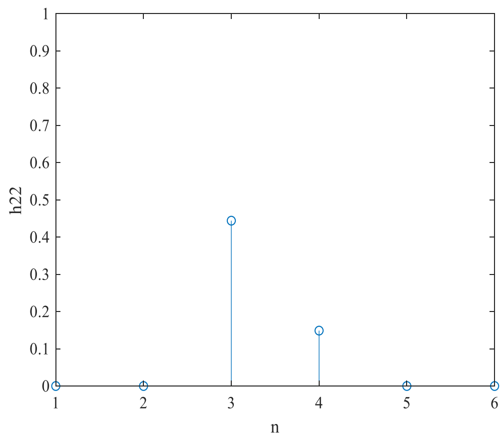

(d)

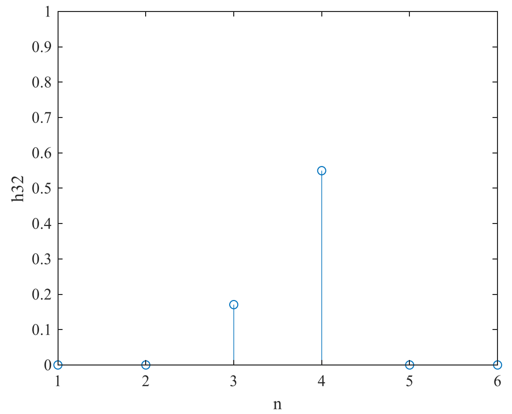

(e)

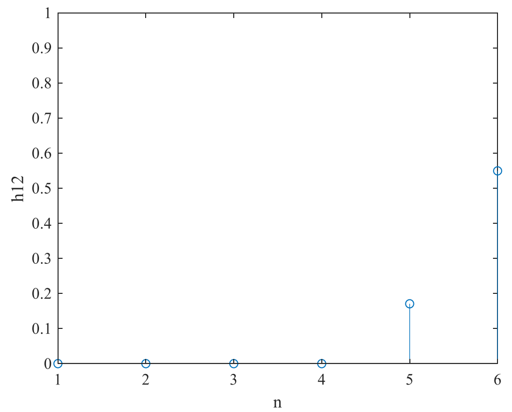

(f)

Figure 19. The impulse response of the MIMO channel

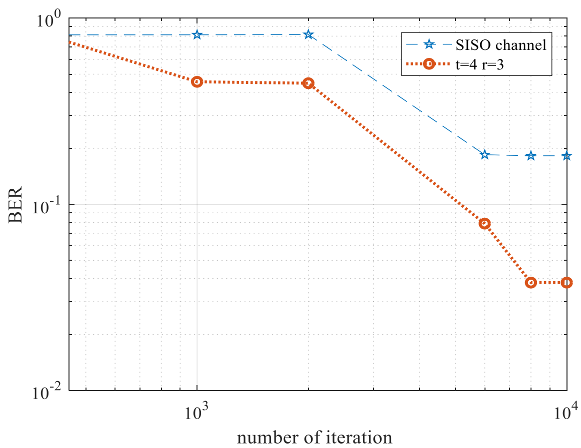

Figure 20. The variation of the BER according to the number of iterations is based on the MIMO-SOSA algorithm with QOSTBC code for (t = 1, r = 1), and (t = 4, r = 3), for MIMO fading channels

In this section of the simulation, we choose to t = 2, r = 3, and SNR = 10 dB. The equalizer impulse responses are shown in Figures 18; which depict the impulse response of the equalizer system after 10,000 iterations. From this figure, the MIMO-SOSA equalizer is able to recover the second input signal, remove ISI. The channel impulse responses are shown in Figure 19.

In this simulation example, it shows t = 3 and r = 2. The channel impulse responses are shown and SNR = 10dB.

We make the last simulation to study the convergence of the SOSA-MIMO algorithm, where we use the Rayleigh fading channel with the use of 3 antennas at the receiver and 3 at the transmitter and SNR=10dB, and we try to study the change of the BER according to the number of iterations n. Figure 20 shows notice when the number of iterations becomes close to 100000 iterations, the converges of this equalizer toward the best results. So the SOSA-MIMO algorithm converges faster than other algorithms.

7. CONCLUSION

It gives practically the same performances for the different numbers of antennae it is interesting to note that the number of channels in the MIMO-SOSA system is caused by the convergence of the BER curves as a function of SNR when the number of antennas in the MIMO-SOSA system increases the MIMO-SOSA algorithm gives the best performance of the MIMO channels. This is natural since the ISI exists. The MIMO-SOSA on the other hand is limited ISI. Hence, by proper initialization, the SOSA-MIMO blind equalizer can be used in MIMO communication systems to recover the desired signal, remove inter-symbol interference, and suppress co-channel interference and adjacent channel interference. With the increase in the number of antennas showed the effectiveness of this blind equalization with QOSTBC coding which proves the advantage of use in wireless communications. Will be noted that the larger the number of antennas the weaker the presence of BER, which shows that the convergence of the algorithm is fast and increases the number of the antenna. This proves that by using this algorithm we can improve the receiver given an improvement in the quality of wireless communication. It can be observed that this algorithm also does a good job on the parameters to compensate for the effect of the channel. These results show the performance and quality.

REFERENCES

[1] Asif, R.M., Arshad, J., Shakir, M., Noman, S.M., Rehman, A.U. (2020). Energy efficiency augmentation in massive MIMO systems through linear precoding schemes and power consumption modeling. Wireless Communications and Mobile Computing, 2020(1): 8839088. https://doi.org/10.1155/2020/8839088

[2] Shang, B., Liu, L., Chen, H., Zhang, C.J., Pudlewski, S., Bentley, E.S., Ashdown, J.D. (2020). Spatial spectrum sensing in uplink two-tier user-centric deployed HetNets. IEEE Transactions on Wireless Communications, 19(12): 7957-7972. https://doi.org/10.1109/TWC.2020.3018408

[3] Khare, A., Trivedi, K., Dixit, S. (2014). Effect of Doppler frequency and BER in FFT based OFDM system with Rayleigh fading channel. In 2014 IEEE Students' Conference on Electrical, Electronics and Computer Science, Bhopal, India, pp. 1-6. https://doi.org/10.1109/SCEECS.2014.6804500

[4] Loss, D.V., Decastro, M.C.F., Franco, P.R.G., Decastro, F.C.C. (2007). Phase transmittance RBF neural networks. IEEE Electronics Letters, 43(16): 882-884. http://doi.org/10.1049/el:20070016

[5] Zerdoumi, Z., Chikouche, D., Benatia, D. (2013). Adaptive decision feedback equalizer based neural

network for nonlinear channels. In 3rd International Conference on Systems and Control, Algiers, Algeria, pp. 850-855. https://doi.org/10.1109/ICoSC.2013.6750956
[6] Chen, S. (2003). Low complexity concurrent constant modulus algorithm and soft decision directed scheme for blind equalisation. IEE Proceedings-Vision, Image and Signal Processing, 150(5): 312-320.
[7] Sahoo, H.K., Mohanty, B. (2016). Adaptive decision feedback equalizer for SISO communication channel using combined FIR-neural network and fast block LMS algorithm. In 2016 IEEE Annual India Conference (INDICON), Bangalore, India, pp. 1-5. https://doi.org/10.1109/INDICON.2016.7839048
[8] Das, S. (2008). Design of adaptive channel equaliser on neural framework using fuzzy logic based multilevel sigmoid slope adaptation. In 2008 International Conference on Signal Processing, Communications and Networking, Chennai, India, pp. 274-278. https://doi.org/10.1109/ICSCN.2008.4447203
[9] Haykin, S.S. (1996). Adaptive filter theory. Pearson Education India. Prentice-Hall, Upper Saddle River, NJ, USA, 3rd edition, 1996.
[10] Jfoschini, G. (1998). On limits of wireless communication in a fading environment when using multiple antennas. Wireless Personal Communications, 6(3): 311-335.
[11] Telatar, E. (1999). Capacity of multi-antenna Gaussian channels. European Transactions on Telecommunications, 10(6): 585-595. https://doi.org/10.1002/ett.4460100604
[12] Nandi, S., Pathak, N.N., Nandi, A. (2020). A novel adaptive optimized fast blind channel estimation for cyclic prefix assisted space–time block coded MIMO-OFDM systems. Wireless Personal Communications, 115(2): 1317-1333. https://doi.org/10.1007/s11277-020-07629-z
[13] Yang, R.N., Zhang, W.T., Lou, S.T. (2020). Joint adaptive blind channel estimation and data detection for MIMO-OFDM systems. Wireless Communications and Mobile Computing, 2020(1): 2508130. https://doi.org/10.1155/2020/2508130
[14] Hong, X., Gao, J., Chen, S. (2020). Semi-blind joint channel estimation and data detection on sphere manifold for MIMO with high-order QAM signaling. Journal of the Franklin Institute, 357(9): 5680-5697. https://doi.org/10.1016/j.jfranklin.2020.04.009
[15] Kimothi, M., Gupta, V.K. (2015). A review of blind channel estimation in MIMO OFDM. International Journal of Advanced Research in Computer and Communication Engineering, 4(5): 72-73. https://doi.org/10.17148/IJARCCE.2015.4516
[16] Ko, K., Lee, J., Shin, W. (2021). Joint power allocation and scheduling techniques for BER minimization in multiuser MIMO systems. IEEE Access, 9: 66675-66686. https://doi.org/10.1109/ACCESS.2021.3074980
[17] Dilli, R. (2021). Performance analysis of multi user massive MIMO hybrid beamforming systems at millimeter wave frequency bands. Wireless Networks, 27(3): 1925-1939. https://doi.org/10.1007/s11276-021-02546-w
[18] Jamali, V., Tulino, A.M., Fischer, G., Müller, R.R., Schober, R. (2020). Intelligent surface-aided transmitter architectures for millimeter-wave ultra massive MIMO systems. IEEE Open Journal of the Communications Society, 2: 144-167. https://doi.org/10.1109/OJCOMS.2020.3048063
[19] Alamouti, S.M. (1998). A simple transmit diversity technique for wireless communications. IEEE Journal on Selected Areas in Communications, 16(8): 1451-1458. https://doi.org/10.1109/49.730453
[20] Jafarkhani, H. (2001). A quasi-orthogonal space-time block code. IEEE Transactions on Communications, 49(1): 1-4. https://doi.org/10.1109/26.898239
[21] Su, W., Xia, X.G. (2004). Signal constellations for quasi-orthogonal space-time block codes with full diversity. IEEE Transactions on Information Theory, 50(10): 2331-2347. https://doi.org/10.1109/TIT.2004.834740
[22] He, B., Su, H., Huang, J. (2021). Joint beamforming and power allocation between a multistatic MIMO radar network and multiple targets using game theoretic analysis. Digital Signal Processing, 115: 103085. https://doi.org/10.1016/j.dsp.2021.103085
[23] Li, F., Jiang, Y., Du, C., Wang, X. (2021). Construction of Golay complementary matrices and its applications to MIMO omnidirectional transmission. IEEE Transactions on Signal Processing, 69: 2100-2113. https://doi.org/10.1109/TSP.2021.3067467
[24] Temiz, M., Alsusa, E., Baidas, M.W. (2020). A dual-functional massive MIMO OFDM communication and radar transmitter architecture. IEEE Transactions on Vehicular Technology, 69(12): 14974-14988. https://doi.org/10.1109/TVT.2020.3031686
[25] Majumder, M., Saxena, H., Srivastava, S., Jagannatham, A.K. (2021). Optimal bit allocation-based hybrid precoder-combiner design techniques for mmWave MIMO-OFDM systems. IEEE Access, 9: 54109-54125. https://doi.org/10.1109/ACCESS.2021.3070921
[26] Yerrapragada, A.K., Kelley, B. (2020). On the application of K-user MIMO for 6G enhanced mobile broadband. Sensors, 20(21): 6252. https://doi.org/10.3390/s20216252
[27] Guerreiro, J., Dinis, R., Campos, L. (2020). On the achievable capacity of MIMO-OFDM systems in the CathLab environment. Sensors, 20(3): 938. https://doi.org/10.3390/s20030938
[28] Saad, W., Bennis, M., Chen, M. (2019). A vision of 6G wireless systems: Applications, trends, technologies, and open research problems. IEEE Network, 34(3): 134-142. https://doi.org/10.1109/MNET.001.1900287
[29] Mayer, K.S., Moreira, V.R., Soares, J.A., Arantes, D.S. (2020). High data-rates and high-order DP-QAM optical links can be efficiently implemented with concurrent equalization. In 2020 Photonics North (PN), Niagara Falls, ON, Canada, pp. 1-1. https://doi.org/10.1109/PN50013.2020.9167008
[30] Mayer, K.S., Müller, C., de Castro, F.C.C., de Castro, M.C.F. (2019). A new CPFSK demodulation approach for software defined radio. Journal of Circuits, Systems and Computers, 28(14): 1950243. https://doi.org/10.1142/S0218126619502438
[31] Li, Y., Lin, K.R. (1996). On blind equalization of MIMO channels. In Proceedings of ICC/SUPERCOMM'96-International Conference on Communications, Dallas, TX, USA, pp. 1000-1004. https://doi.org/10.1109/ICC.1996.541361
[32] Lázaro, M., Santamaría, I., Erdogmus, D., Hild, K.E., Pantaleón, C., Principe, J.C. (2005). Stochastic blind equalization based on pdf fitting using parzen estimator.

IEEE Transactions on Signal Processing, 53(2): 696-704. https://doi.org/10.1109/TSP.2004.840767

[33] Telatar, E. (1999). Capacity of multi-antenna Gaussian channels. European Transactions on Telecommunications, 10(6): 585-595. https://doi.org/10.1002/ett.4460100604

[34] Elkassimi, S., Safi, S., Manaut, B. (2017). Blind channel equalization by adaptive filter algorithms. Universal Journal of Applied Mathematics, 5(3): 45-52. https://doi.org/10.13189/ujam.2017.050301

[35] Godard, D. (1980). Self-recovering equalization and carrier tracking in two-dimensional data communication systems. IEEE Transactions on Communications, 28(11): 1867-1875. https://doi.org/10.1109/TCOM.1980.1094608

[36] de Carvalho, E., Slock, D.T. (2004). Blind and semi-blind FIR multichannel estimation: (Global) identifiability conditions. IEEE Transactions on Signal Processing, 52(4): 1053-1064. https://doi.org/10.1109/TSP.2004.823504

[37] Shalvi, O., Weinstein, E. (1990). New criteria for blind deconvolution of nonminimum phase systems (channels). IEEE Transactions on Information Theory, 36(2): 312-321. https://doi.org/10.1109/18.52478

[38] Porat, B., Friedlander, B. (1991). Blind equalization of digital communication channels using high-order moments. IEEE Transactions on Signal Processing, 39(2): 522-526. https://doi.org/10.1109/78.80846

[39] Boulouird, M., Hassani, M.M., Zeroual, A. (2008). Blind channel identification using higher-order statistics. Journal of Statistical Computation and Simulation, 78(4): 325-338. https://doi.org/10.1080/00949650601081835

[40] Fijalkow, I., Manlove, C.E., Johnson, C.R. (1998). Adaptive fractionally spaced blind CMA equalization: Excess MSE. IEEE Transactions on Signal Processing, 46(1): 227-231. https://doi.org/10.1109/78.651224

[41] Cho, Y.S., Kim, J., Yang, W.Y., Kang, C.G. (2010). MIMO-OFDM Wireless Communications with MATLAB. John Wiley & Sons.

[42] Bendoukha, S., Daas, A., Weiss, S. (2009). Blind adaptive equalizer for broadband MIMO STBC based on PDF fitting. In 2009 17th European Signal Processing Conference, Glasgow, UK, pp. 2643-2647.

[43] Jafarkhani, H., Hassanpour, N. (2005). Super-quasi-orthogonal space-time trellis codes for four transmit antennas. IEEE Transactions on Wireless Communications, 4(1): 215-227. https://doi.org/10.1109/TWC.2004.840247

[44] Proakis, J.G., Salehi, M. (2008). Digital Communications. McGraw-Hill Higher Education.

[45] Soares, J.A., Mayer, K.S., de Castro, F.C.C., Arantes, D.S. (2021). Complex-valued phase transmittance RBF neural networks for massive MIMO-OFDM receivers. Sensors, 21(24): 8200. https://doi.org/10.3390/s21248200